JACS
JOURNAL OF THE AMERICAN CHEMICAL SOCIETY
Article
pubs.acs.org/JACS

Interplay of Metalloligand and Organic Ligand to Tune Micropores within Isostructural Mixed-Metal Organic Frameworks (M′MOFs) for Their Highly Selective Separation of Chiral and Achiral Small Molecules

Madhab C. Das,[†] Qunsheng Guo,[†] Yabing He,[†] Jaheon Kim,[‡] Cong-Gui Zhao,[†] Kunlun Hong,[δ] Shengchang Xiang,[†,⊥] Zhangjing Zhang,[†,⊥] K. Mark Thomas,[∥] Rajamani Krishna,*[,#] and Banglin Chen*[,†]

[†]Department of Chemistry, University of Texas at San Antonio, One UTSA Circle, San Antonio, Texas 78249-0698, United States
[‡]Department of Chemistry, Soongsil University, Seoul 156-743, Korea
[δ]Center for Nanophase Materials Sciences, Oak Ridge National Laboratory, Oak Ridge, Tennessee 37831, United States
[⊥]College of Chemistry and Materials, Fujian Normal University, 3 Shangsan Road, Cangshang Region, Fuzhou, China 350007
[∥]Northern Carbon Research Laboratories, Sir Joseph Swan Institute for Energy Research and School of Chemical Engineering and Advanced Materials, University of Newcastle upon Tyne, Bedson Building, Newcastle upon Tyne, NE1 7RU, U.K.
[#]Van 't Hoff Institute for Molecular Sciences, University of Amsterdam, Science Park 904, 1098 XH Amsterdam, The Netherlands

Supporting Information

ABSTRACT: Four porous isostructural mixed-metal−organic frameworks (M′MOFs) have been synthesized and structurally characterized. The pores within these M′MOFs are systematically tuned by the interplay of both the metalloligands and organic ligands which have enabled us not only to direct their highly selective separation of chiral alcohols 1-phenylethanol (PEA), 2-butanol (BUT), and 2-pentanol (2-PEN) with the highest ee up to 82.4% but also to lead highly selective separation of achiral C_2H_2/C_2H_4 separation. The potential application of these M′MOFs for the fixed bed pressure swing adsorption (PSA) separation of C_2H_2/C_2H_4 has been further examined and compared by the transient breakthrough simulations in which the purity requirement of 40 ppm in the outlet gas can be readily fulfilled by the fixed bed M′MOF-**4a** adsorber at ambient conditions.

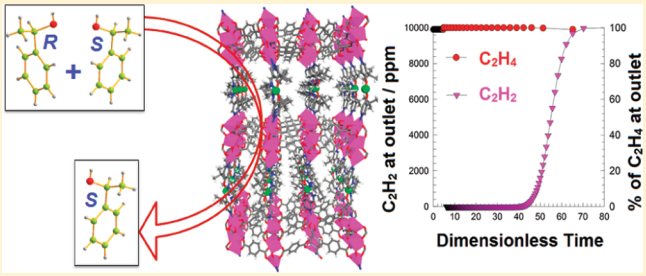

INTRODUCTION

The last two decades have witnessed the rapid emerge of porous metal−organic frameworks (MOFs) and/or porous coordination polymers (PCPs) and their diverse applications on gas storage, separation, heterogeneous catalysis, sensing, drug delivery, and so on.[1,2] The so-called first-generation MOF/CP materials is structurally porous (guest solvent molecules occupy the pore spaces within the frameworks); however, their permanent porosity cannot be established by vapor/gas sorption because the frameworks are not robust enough and easily collapsed once the solvent molecules are removed during thermal and/or vacuum activation.[3−6] Significant progress was made during 1997−1999 when a few highly porous MOFs were synthesized that adsorbed gas molecules.[7−9] The realization of such robust second-generation MOF/CP materials has certainly paved the way to explore their functionalities and thus further to target third-generation MOF/CP materials which can respond to physical stimuli, leading to a variety of new porous materials for the above-mentioned applications.[10−74] In fact, MOF materials have been the best performing of all porous materials for the storage of hydrogen, methane, and acetylene and capture of carbon dioxide that have been produced over the past several years.[18−24]

During the early stage, research was mainly focused on those commercially available organic ligands such as 4,4′-bipyridyl to construct frameworks.[6,7,10] The realization of carboxylate groups for stabilization of frameworks by the in situ formation of metal-containing clusters (generally termed as secondary building units (SBUs)) during 1998−1999 has significantly facilitated the production of robust and/or robust/flexible porous MOFs,[12] and further stimulated the exploration of the decorated and expanded carboxylate-containing organic linkers for the construction of highly porous MOFs, as exemplified in MOF-11 and MOF-14 by the implementation of 1,3,5,7-admantane-tetracarboxylate (ATC) and 4,4′,4″-benzene-1,3,5-triyl-tribenzoate (BTB) respectively, into the frameworks

Received: March 19, 2012
Published: April 30, 2012

dx.doi.org/10.1021/ja302380x | J. Am. Chem. Soc. 2012, 134, 8703−8710

during 2000−2001.[50,51] Nowadays, the expanded organic linker approach still plays a crucial role in targeting some highly porous MOFs for their extraordinary gas-storage properties. Metalloligands (metal-containing complexes having the coordination binding sites for their further coordination/binding with the second metal ions and/or clusters) as the potential bridging linkers for the construction of porous mixed-metal−organic frameworks (M′MOFs) was conceptually proposed back in 2002;[52] however, it took quite a long time to establish the first few porous M′MOFs whose permanent porosities have been exclusively established by gas/vapor sorption isotherms.[53−71] Compared with traditional organic ligands, metalloligands are typically longer and more flexible, and thus it is much more difficult and challenging to stabilize the formed frameworks. As highlighted recently, such a metalloligand approach is very appealing to target some functional porous materials because of its straightforward immobilization of functional sites (both metal and organic functional sites) into their frameworks to introduce their specific recognitions of small molecules.[61] Apparently, such promise has not been fully explored, and the research on metalloligands for functional porous M′MOFs is still at the early stage.

Fine tuning of micropores within porous materials is very crucial and important to maximize their size-selective effects and thus to fulfill their specific separation of small molecules. As shown in Scheme 1, through the interplay of both metal-

Scheme 1. Schematic Diagram for the Synthesis of Four Mixed-Metal Organic Frameworks (M′MOFs) of Tunable Chiral Pores by Making Use of Different Diamines (red), Terminal Alkyl Moieties (blue) and Organic Linkers (green)

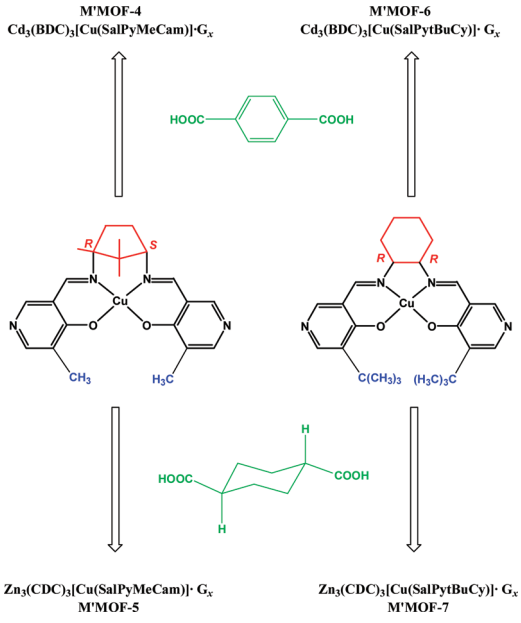

loligands and organic ligands, our developed M′MOF approach is very unique to construct tunable chiral pore spaces for both chiral and achiral separation of small molecules. Simply by making use of different chiral diamines ((1*R*,3*S*)-1,2,2-trimethyl-1,3-diaminocyclopentane and (1*R*,2*R*)-(-)-1,2-cyclohexanediamine; red in Scheme 1), chiral pockets/environments with slightly different pores can be readily constructed. These pores can be further tuned by both the substituted terminal methyl and *tert*-butyl groups (blue in Scheme 1) and the second organic linkers 1,4-cyclohexanedicarboxylate and 1,4-benzenedicarboxylate (green in Scheme 1). Herein we report the synthesis and structures of four isostructural M′MOFs $Cd_3(BDC)_3[Cu(SalPyMeCam)]\cdot(G)_x$ (**M′MOF-4**), $Zn_3(CDC)_3[Cu(SalPyMeCam)]\cdot(G)_x$ (**M′MOF-5**), $Cd_3(BDC)_3[Cu(SalPytBuCy)]\cdot(G)_x$ (**M′MOF-6**) and $Zn_3(CDC)_3[Cu(SalPytBuCy)]\cdot(G)_x$ (**M′MOF-7**), and their chiral separation of small alcohols and separation of C_2H_2/C_2H_4 at room temperature. **M′MOF-7** can efficiently separate 1-phenylethanol up to ee of 82.4. Their potential for the practical separation of C_2H_2/C_2H_4 at ambient conditions has been further examined by simulated breakthrough experiments, indicating that activated **M′MOF-4a** is the best material to produce high purity ethylene (>99.0%) from the C_2H_4/C_2H_2 mixture for industrial usage.

EXPERIMENTAL SECTION

Materials. All reagents and solvents used in these studies are commercially available and were used as received without further purification. 5-Methyl-4-oxo-1,4-dihydro-pyridine-3-carbaldehyde and 5-*tert*-butyl-4-oxo-1,4-dihydro-pyridine-3-carbaldehyde were synthesized according to the published procedure.[75] (1*R*,3*S*)-1,2,2-Trimethyl-1,3-diaminocyclopentane was readily obtained from natural camphoric acid.[76]

Synthesis of $Cu(H_2SalPyMeCam)(NO_3)_2$. A solution of (1*R*,3*S*)-1,2,2-trimethyl-1,3-diaminocyclopentane (0.231 g, 1.5 mmol) in dry MeOH (30 mL) was added dropwise to a solution of 5-methyl-4-oxo-1,4-dihydro-pyridine-3-carbaldehyde (0.412 g, 3.0 mmol) in dry MeOH (100 mL), and the resulting mixture was refluxed for 4 h to form a clear, light-brown solution. To this solution was added a solution of $Cu(NO_3)_2\cdot 2.5H_2O$ (0.350 g, 1.5 mmol) in MeOH (20 mL), and the mixture was stirred for another 6 h at RT. The product was obtained as a bluish green precipitate with 75% yield that was collected by evaporation of solvent under reduced pressure. Elemental analysis (%): Calcd for $Cu(H_2SalPyMeCam)(NO_3)_2(H_2O)_{1.5}$ ($C_{22}H_{31}N_6O_{9.5}Cu$): C, 44.41; H, 5.25; N, 14.12; Found: C, 44.59; H, 5.00; N, 13.68.

Synthesis of $Cu(H_2SalPytBuCy)(NO_3)_2$. A solution of (1*R*,2*R*)-(−)-1,2-cyclohexanediamine (0.231 g, 1.5 mmol) in dry EtOH (30 mL) was added dropwise to a solution of 5-*tert*-butyl-4-oxo-1,4-dihydro-pyridine-3-carbaldehyde (0.504 g, 3.0 mmol) in dry EtOH (100 mL), and the resulting mixture was refluxed for 4 h to form a clear light-brown solution. To this solution was added a solution of $Cu(NO_3)_2\cdot 2.5H_2O$ (0.350 g, 1.5 mmol) in EtOH (20 mL), and the mixture was stirred for another 5 h at RT. The product was obtained as blue precipitate with 50% yield that was collected by filtration, washed with EtOH, and air-dried. Elemental analysis (%): Calcd for $Cu(H_2SalPytBuCy)(NO_3)_2(H_2O)_2$ ($C_{26}H_{40}N_6O_{10}Cu$): C, 47.30; H, 6.10; N, 12.73; Found: C, 46.94; H, 5.30; N, 13.60.

Synthesis of M′MOF-4: $Cd_3(BDC)_3[Cu(SalPyMeCam)]\cdot(DMF)_9(H_2O)_2$. A mixture of $Cu(H_2SalPyMeCam)(NO_3)_2$ (0.018 g, 0.030 mmol), H_2BDC (0.0067 g, 0.04 mmol,) and $Cd(NO_3)_2\cdot 4H_2O$ (0.0123 g, 0.04 mmol) in DMF (3 mL) was sonicated for 10 min and heated in a 20 mL scintillation vial with a screw cap at 120 °C for 24 h. M′MOF-**4** could be isolated in ∼57% yield as green thin plates. Elemental analysis (%): Calcd for $Cd_3(BDC)_3[Cu(SalPyMeCam)]\cdot(DMF)_9(H_2O)_2$ ($C_{73}H_{105}N_{13}O_{25}CuCd_3$): C, 44.61; H, 5.38; N, 9.26; Found: C, 44.60; H, 5.16; N, 9.02.

Synthesis of M′MOF-5: $Zn_3(CDC)_3[Cu(SalPyMeCam)]\cdot(DMF)_5(H_2O)_7$. When $Zn(NO_3)_2$ (0.0120 g, 0.04 mmol) and H_2CDC (0.0069 g, 0.04 mmol) were taken in place of $Cd(NO_3)_2\cdot 4H_2O$ and H_2BDC respectively, keeping the reaction conditions the same as in M′MOF-**4**, M′MOF-**5** could be isolated in ∼60% yield as green thin plates. Elemental analysis (%): Calcd for $Zn_3(CDC)_3[Cu(SalPyMeCam)]\cdot(DMF)_5(H_2O)_7$ ($C_{61}H_{99}N_9O_{26}CuZn_3$): C, 44.83; H, 6.11; N, 7.71; Found: C, 45.04; H, 6.12; N, 7.69.

dx.doi.org/10.1021/ja302380x | *J. Am. Chem. Soc.* 2012, 134, 8703−8710

Synthesis of M′MOF-6: $Cd_3(BDC)_3[Cu(SalPytBuCy)]\cdot(DMF)_{10}$. A mixture of $Cu(H_2SalPytBuCy)(NO_3)_2$ (0.015 g, 0.023 mmol), H_2BDC (0.0067 g, 0.04 mmol), and $Cd(NO_3)_2\cdot 4H_2O$ (0.0123 g, 0.04 mmol) in DMF (3 mL) was sonicated for 10 min and heated in a 20 mL scintillation vial with a screw cap at 100 °C for 48 h. Dark-blue thin plate crystals of M′MOF-**6** were collected, washed with DMF, and dried in air with 55% yield. Elemental analysis (%): Calcd for $Cd_3(BDC)_3[Cu(SalPytBuCy)]\cdot(DMF)_{10}$ ($C_{80}H_{115}N_{14}O_{24}CuCd_3$): C, 46.69; H, 5.63; N, 9.53; Found: C, 47.00; H, 5.40; N, 9.67.

Synthesis of M′MOF-7: $Zn_3(CDC)_3[Cu(SalPytBuCy)]\cdot(DMF)_{12}(H_2O)_6$. When $Zn(NO_3)_2$ (0.0120 g, 0.04 mmol) and H_2CDC (0.0069 g, 0.04 mmol) were taken in place of $Cd(NO_3)_2\cdot 4H_2O$ and H_2BDC respectively, keeping the reaction conditions the same as the above, M′MOF-7 could be isolated in ∼53% yield as dark-blue thin plates. Elemental analysis (%): Calcd for $Zn_3(CDC)_3[Cu(SalPytBuCy)]\cdot(DMF)_{12}(H_2O)_6$ ($C_{86}H_{160}N_{16}O_{32}CuZn_3$): C, 47.16; H, 7.36; N, 10.23; Found: C, 47.27; H, 6.68; N, 10.40.

Single-Crystal Studies. Crystal structure determination was carried out using a Bruker SMART APEX2 CCD-based X-ray diffractometer equipped with a low-temperature device and Mo-target X-ray tube (wavelength = 0.71073 Å). Data collection, indexing, and initial cell refinements were carried out using APEX2; frame integration and final cell refinements were done using SAINT. The molecular structure of the compound was determined using direct methods and Fourier techniques, and was refined by full-matrix least-squares. An absorption correction, including face-indexed absorption correction, was applied using the program SADABS. All non-hydrogen atoms were refined anisotropically (except as noted). For M′MOF-**4**, two independent half metalloligand moieties are disordered over two sites with sof of 0.5, respectively, which required geometrical restraints on the bond distances. In addition, the temperature factors of some atoms (C36′, C51′, C54, C56−C60) were refined with applying EADP instructions. Non-hydrogen atoms were refined anisotropically except for the C, N, and O atoms of the disordered metalloligand moieties. The final refinement process converged to R1 = 0.0808 ($I > 2\sigma(I)$). The occluded solvent molecules could not be identified clearly with the current intensity data, which needed PLATON SQUEEZE calculations. Using the new data without the solvent contribution, the final refinement process converged to R1 = 0.0673 ($I > 2\sigma(I)$). Due to the disorder of the metalloligand, Flack's absolute parameter could not converge to 0. However, the low value, 0.10, indicates that the absolute configuration of the Salen in the framework corresponds to the absolute configuration of the starting compound.

Physical Measurements. Thermogravimetric analyses (TGA) were performed with a Shimadzu TGA-50 analyzer under nitrogen atmosphere with a heating rate of 3 °C min^{-1}, from 22−900 °C. X-ray powder patterns were measured with a Rigaku Ultima IV diffractometer at 40 kV, 40 mA for Cu Kα radiation (λ = 1.5418 Å), with a scan rate of 3 deg min^{-1}. The elemental analyses were performed with Perkin−Elmer 240 CHN Analyzers from Galbraith Laboratories Inc., Knoxville, TN. A Micromeritics ASAP 2020 surface area analyzer was used to measure gas adsorption isotherms. In order to have guest-free frameworks, the fresh sample soaked in methanol (exchanged at least 15 times) was filtered and vacuumed at room temperature overnight until the outgas rate was 5 μmHg min^{-1} prior to measurements. The temperature of the samples was maintained at 77 K with liquid nitrogen, 273 K with ice−water bath (slush), and 296 K with a water bath.

Chiral HPLC Analysis. As-synthesized M′MOF **4**−**7** samples were exchanged with dry MeOH for several times. The MeOH-exchanged samples were immersed in racemic alcohols in sealed vials at RT for two days, filtered, washed with dry diethyl ether for several times, and transferred to other vials containing dry MeOH. After two days, the liquid containing both MeOH and desorbed alcohols were filtered, and the released alcohols from these alcohol-encapsulated M′MOFs were determined by the chiral HPLC analysis. The enantiomeric excess for the encapsulated 1-PEA in methanol solution was performed on a Chiralcel OD-H column with a flow rate of 0.5 mL/min and an eluent of 95:5 of hexane/isopropanol. Desorbed aliphatic alcohols (2-butanol, 2-pentanol, and 2-heptanol) mixed with MeOH were derivatized with 4-methoxybenzoyl chloride in presence of Et_3N and 4-dimethylaminopyridine (DMAP, used as catalyst) under continuous stirring at RT for 24 h before being subjected to HPLC run (chiralcel OB-H column with a flow rate of 0.5 mL/min and an eluent of 95:5 of hexane/isopropanol was used). The absolute configuration was determined by comparison of their HPLC retention times to those of authentic samples. The experimental data along with HPLC graphs with retention times (t_R) and area percentages for major and minor enantiomers are provided in the Supporting Information (SI). It should be noted that, 4-methoxybenzoyl derivative of MeOH was also formed during the derivatization of desorbed alcohols, and its retention time is much higher than that of either of the enantiomers of desired alcohols.

Fits of Pure Component Isotherms Synthesized in This Study. The measured experimental data on pure component isotherms for C_2H_2 and C_2H_4 at 273 K, and 296 K in the four different M′MOFs were first converted to absolute loadings using the Peng−Robinson equation of state for estimation of the fluid densities. The pore volume data given in Table S1 (SI) were used for this purpose. Depending on the guest−host combination, the choice of the isotherm is either a 1-site Langmuir, 2-site Langmuir, or Langmuir−Freundlich model. The isotherm models selected along with the fit parameters are specified in Tables S2, S3, S4, and S5 (SI).

Isosteric Heat of Adsorption. The isosteric heat of adsorption, Q_{st}, defined as

$$Q_{st} = RT^2\left(\frac{\partial \ln p}{\partial T}\right)_q \qquad (1)$$

were determined using the pure component isotherm fits for the four M′MOFs synthesized in this study. For some guest−host combinations for which either the dual-site Langmuir or Langmuir−Freundlich fits were used, Q_{st} is a function of the loading.[77]

RESULTS AND DISCUSSION

The Schiff base $H_2SalPyMeCam$ was synthesized by the condensation of 5-methyl-4-oxo-1,4-dihydro-pyridine-3-carbaldehyde with (1*R*,3*S*)-1,2,2-trimethyl-1,3-diaminocyclopentane; while $H_2SalPytBuCy$ was prepared from the reaction of 5-*tert*-butyl-4-oxo-1,4-dihydro-pyridine-3-carbaldehyde with (1*R*,2*R*)-(−)-1,2-cyclohexanediamine. Addition of $Cu(NO_3)_2\cdot 2.5H_2O$ in methanol/ethanol to the in situ-formed Schiff base $H_2SalPyMeCam$ and $H_2SalPytBuCy$ in methanol/ethanol readily formed the metalloligand precursors $Cu(H_2SalPyMeCam)(NO_3)_2$ and $Cu(H_2SalPytBuCy)(NO_3)_2$, respectively. Solvothermal reactions of these two metalloligand precursors with metal salts ($Cd(NO_3)_2\cdot 4H_2O$ or $Zn(NO_3)_2\cdot 6H_2O$) and the second organic linkers 1,4-benzenedicarboxylic acid (H_2BDC) or 1,4-cyclohexanedicarboxylic acid (H_2CDC) in DMF led to the formation of four M′MOFs. They were formulated as $Cd_3(BDC)_3[Cu(SalPyMeCam)]\cdot(DMF)_9(H_2O)_2$ (M′MOF-**4**), $Zn_3(CDC)_3[Cu(SalPyMeCam)]\cdot(DMF)_5(H_2O)_7$ (M′MOF-**5**), $Cd_3(BDC)_3[Cu(SalPytBuCy)]\cdot(DMF)_{10}$ (M′MOF-**6**), and $Zn_3(CDC)_3[Cu(SalPytBuCy)]\cdot(DMF)_{12}(H_2O)_6$ (M′MOF-**7**) based on elemental analyses and single-crystal X-ray studies. The phase purity of the bulk samples was further confirmed by powder X-ray (PXRD, Figures S1, S3−S4, S6, SI) and thermal gravimetric analysis (TGA, Figures S7−S10, SI). The crystalline products once formed are insoluble in most of the common organic solvents.

Single-crystal X-ray diffraction study shows that these M′MOFs are isostructural, so two representative ones (M′MOF-**4** and M′MOF-**6**) are fully characterized.[78] As shown in Figure 1 for the structure of M′MOF-**6**, these

dx.doi.org/10.1021/ja302380x | J. Am. Chem. Soc. 2012, 134, 8703−8710

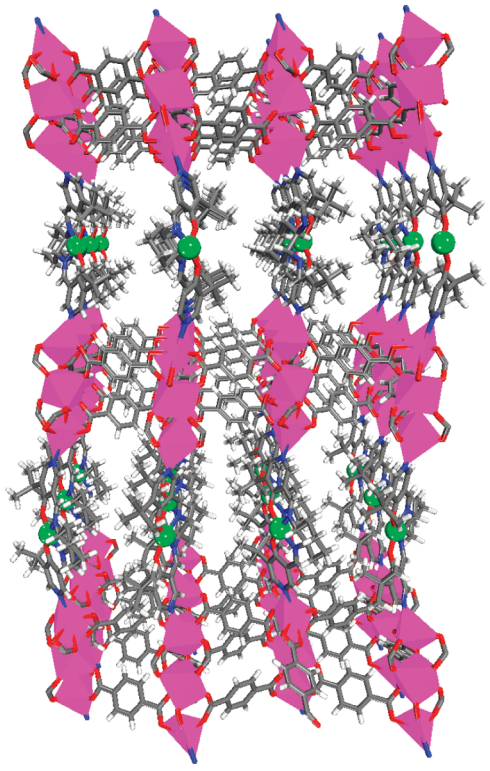

Figure 1. Single crystal structure of **M′MOF-6** viewed along *a* axis (Cu, green; C, gray; H, white; N, blue; O, red; Cd, pink).

M′MOFs exhibit three-dimensional (3D) porous structures. The 2D sheets (see SI, Figure S11) of $Cd_3(BDC)_3$ or $Zn_3(CDC)_3$ are bridged by metalloligands Cu(SalPyMeCam) or Cu(SalPytBuCy) to form 3D frameworks with hexagonal primitive nets (point symbol $3^6.4^{18}.5^3.6$).[83] The chiral pore spaces within the frameworks encapsulate a significant amount of disordered DMF and H_2O solvent molecules.

The chiral porous natures of M′MOF **4**−**7** have enabled us to examine their potential for enatioselective separation of small alcohols 1-phenylethanol (1-PEA), 2-butanol (2-BUT), 2-pentanol (2-PEN), and 2-heptanol (2-HEP) at room temperature (Scheme 2). The MeOH-exchanged M′MOF **4**−**7** were

Scheme 2. Enantiopure M′MOFs for the Chiral Resolution of Four Alcohols

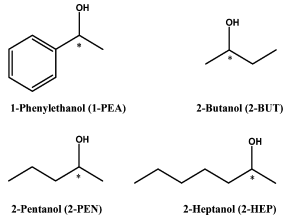

immersed in racemic alcohols, filtered, and washed with diethyl ether. The released alcohols from these alcohol-encapsulated M′MOFs were determined by the chiral HPLC analysis (Figures S12−S28, SI). As shown in Table 1, these porous M′MOFs display different recognition behaviors for these four small alcohols. The two M′MOFs constructed from CDC M′MOF-**5** and M′MOF-**7** systematically exhibit higher chiral separation for 1-phenylethanol (1-PEA) with ee of 75.3% and 82.4%, respectively, than those assembled from BDC M′MOF-**4**

Table 1. Resolution of Chiral Alcohols by M′MOF 4−7

M′MOF	ee[a] (%) for 1-PEA	ee[b] (%) for 2-BUT	ee[b] (%) for 2-PEN	ee[b] (%) for 2-HEP
4	45.0	45.2	27.9	<4
5	75.3	72.5	62.2	<9
6	46.2	49.6	39.7	<6
7	82.4	77.1	65.9	<10

[a]Determined by chiral HPLC analysis using a Chiralcel OD-H column. [b]Determined by chiral HPLC analysis using Chiralcel OB-H column (desorbed aliphatic alcohols were derivatized with 4-methoxybenzoyl chloride before being subjected to the HPLC run).

(ee of 45.0%) and M′MOF-**6** (ee of 46.2%). M′MOF-**7** is the most efficient material for separation of 1-PEA, because of the larger terminal *tert*-butyl group in M′MOF-**7**, which has further decreased the chiral pore space. Such systematic trends have been also observed in these enantiopure M′MOFs for the chiral separation of 2-butanol (2-BUT) and 2-pentanol (2-PEN). It needs to be mentioned that such M′MOFs are flexible with pores that can be modified by adsorption of different solvent substrates (see SI, Figure S2−S3, S5−S6 for their PXRDs in different alcohols); their pores can be slightly adjusted to match and maximize their chiral separation of the 1-PEA, 2-BUT, and 2-PEN.

M′MOFs can be easily regenerated simply by the immersion into excess dry methanol, and thus can be reused for further resolution of racemic alcohols for the next cycles with retention of crystallinity but with a small decrease in enantioselectivity. The high separation capacities of M′MOF-**5** and M′MOF-**7** for their chiral separation of the 1-PEA, 2-BUT, and 2-PEN with the ee up to 82.4% highlight their potential for their practical usage. It has been well-known that chiral secondary alcohols are valuable intermediates in the synthesis of a variety of pharmaceutical, agricultural, and fine chemicals, and thus separation of enantiopure chiral secondary alcohols is very important. As established before,[60] these alcohols are expected not to specifically interact with frameworks, but are located inside the chiral pore spaces, leading to the highly selective enantioselective separation of the examined alcohols by the homochiral M′MOFs. Extensive research endeavors have been pursued to construct porous enantiopure metal−organic frameworks; however, the progress to target their highly selective separation for chiral small molecules has been very slow.[14,39−49,60] The M′MOF approach developed provides promise for the realization of new porous materials for the highly selective separation of chiral small molecules because of the ability to tune the chiral pores by the interplay of both metalloligands and organic linkers.

Activated M′MOFs **4a**−**7a** have quite different gas sorption properties, because of their different pore space and framework flexibility (Figure 2a). The saturated CO_2 uptakes at 195 K are 152, 113, 66, and 24 cm^3/g, respectively, for M′MOF-**4a**, **-6a**, **-5a**, and **-7a**. Accordingly, their BET surface areas are 602, 369, 202, and 90 m^2/g, while their total saturated pore volumes are 0.289, 0.216, 0.126, and 0.045 $cm^3\ g^{-1}$ for M′MOF **4a**, M′MOF **6a**, M′MOF **5a**, and M′MOF **7a**, respectively. Changing metalloligand from Cu(SalPyMeCam) to Cu(SalPytBuCy) systematically reduces the accessible pore space (see Scheme 1: M′MOF-**4a** vs M′MOF-**6a**, M′MOF-**5a** vs M′MOF-**7a**), mainly because the bulky *tert*-butyl groups ($-C(CH_3)_3$) have occupied more pore space in the less porous M′MOF-**6a** and M′MOF-**7a**. BDC is apparently more rigid than CDC; thus,

dx.doi.org/10.1021/ja302380x | *J. Am. Chem. Soc.* 2012, 134, 8703−8710

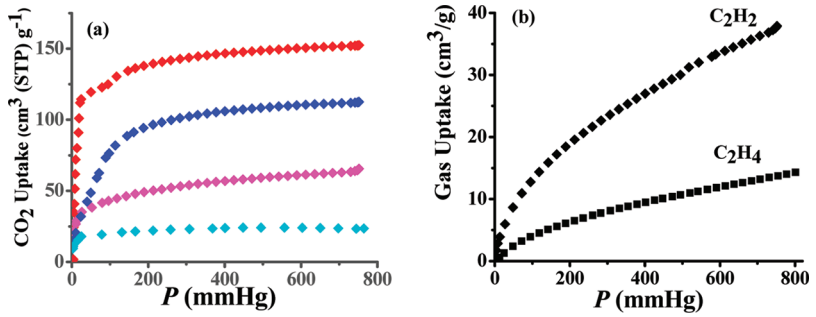

Figure 2. (a) CO_2 adsorption isotherm of M′MOFs at 196 K (M′MOF-**4a**, red; M′MOF-**6a**, blue; M′MOF-**5a**, magenta; M′MOF-**7a**, cyan). (b) C_2H_2 and C_2H_4 adsorption isotherms of M′MOF-**6a** at 295 K.

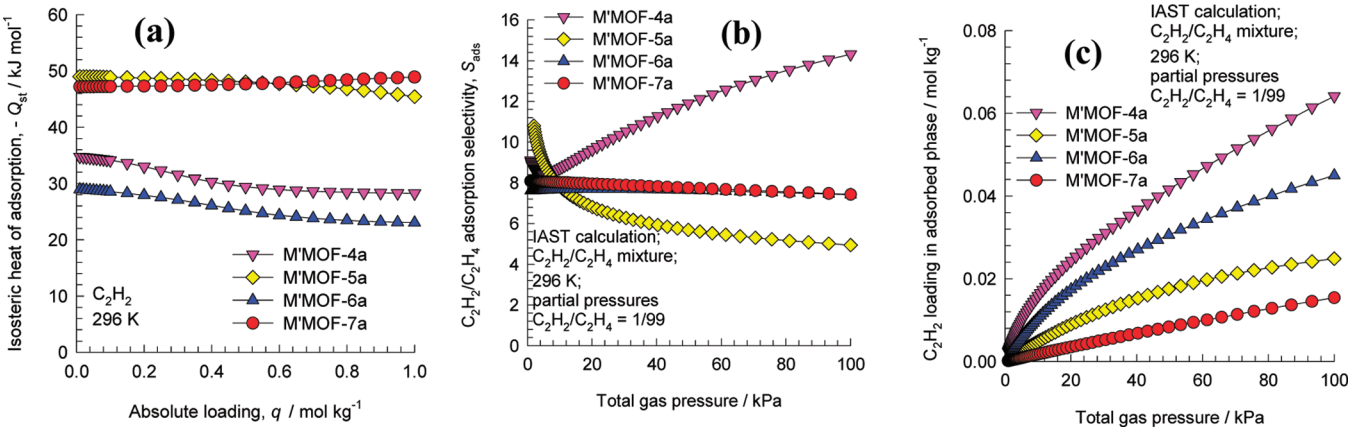

Figure 3. (a) Comparison of the loading dependence of the isosteric heats of adsorption of C_2H_2 in four different M′MOFs. (b) C_2H_2/C_2H_4 adsorption selectivity for the variety of M′MOFs and (c) C_2H_2 uptake capacity, expressed as moles per kg of adsorbent, in equilibrium with a binary C_2H_2/C_2H_4 gas mixture maintained at isothermal conditions at 296 K. In these calculations the partial pressures of C_2H_2 and C_2H_4 are taken to be: p_1 = 1 kPa; p_2 = 99 kPa. All calculations are for 296 K, using the *T*-dependent isotherm parameters reported in Tables S2−S5 (SI). The calculations are based on the Ideal Adsorbed Solution Theory (IAST) of Myers and Prausnitz.[79].

BDC is better than CDC in terms of its ability to stabilize the frameworks and thus generate more porous M′MOF-**4a** (vs M′MOF-**5a**) and M′MOF-**6a** (vs M′MOF-**7a**).

As shown in Figure 2b and Figures S29−S32 (SI), these porous M′MOFs are very promising for the selective separation of ethylene and acetylene at room temperature. The C_2H_2 uptakes for these M′MOFs are systematically higher than C_2H_4 ones at ambient conditions, establishing the foundation for their applications on C_2H_2/C_2H_4 separation. Based on these temperature dependent sorption isotherms, we have fitted their single component sorption isotherms by the well established 1-site Langmuir, 2-site Langmuir, or Langmuir−Freundlich model (Tables S2−S5, [SI]) and calculated their isosteric heat of adsorption Q_{st}. The loading dependence of Q_{st} for C_2H_2 in different M′MOFs is compared in Figure 3a. The highest values of Q_{st} are for M′MOF-**5a**, and M′MOF-**7a**, with much lower values for M′MOF-**4a**, and M′MOF-**6a**. These are in agreement with their porosities in which the smaller pores will have stronger interactions with acetylene. Using the pure component isotherm fits, the adsorption selectivities were determined using the Ideal Adsorbed Solution Theory (IAST) of Myers and Prausnitz.[79] The accuracy of the IAST calculations for estimation of the component loadings for several binary mixtures in a wide variety of zeolites and for MOFs has been established by comparison with Configurational-Biast Monte Carlo (CBMC) simulations of mixture adsorption.[80] We proceed further to determine the C_2H_2/C_2H_4 adsorption selectivities for the M′MOFs at 296 K. In these calculations the partial pressures of C_2H_2 and C_2H_4 are taken to be: p_1/p_2 = 1/99 (i.e., 1 mol % C_2H_2 in the mixture); see Figure 3b. The highest value of S_{ads} is with M′MOF-**4a**; this is followed by M′MOF-**6a**, M′MOF-**7a**, and M′MOF-**5a**.

Besides selectivity, capacity considerations are important in determining the performance of any given adsorbent in a pressure swing adsorption (PSA) unit. The loadings of C_2H_2 in the adsorbed phase within the M′MOFs in equilibrium with a binary C_2H_2/C_2H_4 gas mixture maintained at isothermal conditions at 296 K were determined for a range of total pressures up to 100 kPa. Figure 3c presents the C_2H_2 uptake capacity, expressed as moles per kg of adsorbent. For the entire range of pressures, the highest uptake capacity of these porous materials is offered by M′MOF-**4a**. It is interesting to note that M′MOF-**4a** scores highly both on *selectivity* and *capacity consideration*. The lowest C_2H_2 uptake capacity is by M′MOF-**7a** because of its less porous nature. Now the key question is: Which of the M′MOFs has the best C_2H_2/C_2H_4 separation characteristics in a PSA unit in order to meet the specified purity level of 40 ppm in the outlet gas? To provide an answer, we need to consider breakthrough characteristics in a packed bed adsorber.

Figure 4a shows a schematic of a packed bed adsorber. The breakthrough calculations were performed using the following methodologies developed and described in earlier works.[81] Assuming plug flow of C_2H_2/C_2H_4 gas mixture through a fixed bed maintained under isothermal conditions and negligible pressure drop, the partial pressures in the gas phase at any

dx.doi.org/10.1021/ja302380x | J. Am. Chem. Soc. 2012, 134, 8703−8710

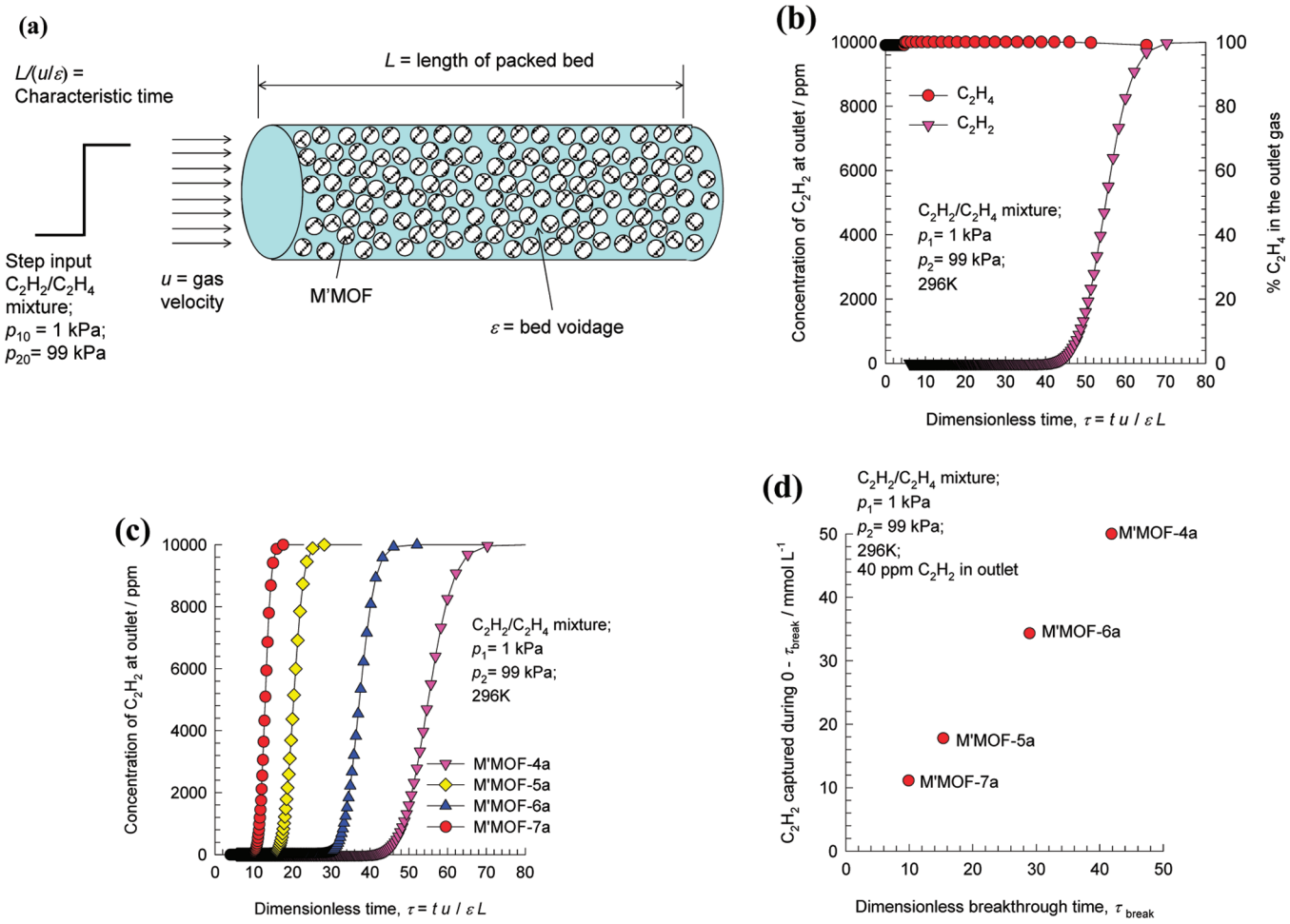

Figure 4. (a) Schematic diagram of a packed bed adsorber. (b) Typical breakthrough curves for packed bed adsorber packed with M′MOF-**4a** with step-input of a 1/99 C_2H_2/C_2H_4 mixture at 296 K and total pressures of 100 kPa. (c) Ppm C_2H_2 in outlet gas as a function of the dimensionless time for M′MOFs. (d) Plot of the number of millimoles of C_2H_2 captured per liter of adsorbent material during the time interval $0-\tau_{break}$ against the breakthrough time τ_{break} for packed bed adsorber with step-input of a 1/99 C_2H_2/C_2H_4 mixture at 296 K and total pressures of 100 kPa. The breakthrough times, τ_{break}, correspond to those when the outlet gas contains 40 ppm C_2H_2.

position and instant of time are obtained by solving the following set of partial differential equations for each of the species i in the gas mixture.

$$\frac{1}{RT}\varepsilon\frac{\partial p_i}{\partial t} = -\frac{1}{RT}\frac{\partial(up_i)}{\partial z} - (1-\varepsilon)\rho\frac{\partial q_i}{\partial t};\ i = 1, 2 \qquad (2)$$

In eq 2, t is the time, z is the distance along the adsorber, ρ is the framework density, ε is the bed voidage (ε = 1− (Bulk density)/(Framework density)), and u is the superficial gas velocity. The molar loadings of the species i, q_i, at any position z, and time t is determined from IAST calculations. Details of the numerical procedures used are available in earlier works.[81,82] In their breakthrough calculation the following parameter values were used: L = 0.12 m; ε = 0.75; u = 0.00225 m/s (at inlet). This implies the volume of adsorbents remains the same. The total mass of the adsorbents used is governed by the corresponding framework densities.

Figure 4b shows the simulated breakthrough curve of M′MOF-**4a** for the C_2H_2/C_2H_4 separation at 296 K. It is very clear that M′MOF-**4a** can efficiently separate C_2H_2 from the C_2H_2/C_2H_4 mixture at room temperature. The examined four M′MOFs have different separation capacities. Figure 4c compares the outlet gas compositions, expressed in ppm C_2H_2, obtained with different M′MOFs. The x-axis in Figure 4c is a dimensionless time, τ, defined by dividing the actual time, t, by the characteristic time. On the basis of the data in Figure 4c, we can determine the breakthrough time, τ_{break}, that satisfies the required purity level of 40 ppm (which corresponds to the feedstock requirements of the polymerization reactor). A longer τ_{break} is desirable because the frequency of regeneration is reduced. M′MOF-**4a** has the longest breakthrough time, while M′MOF-**7a** has the shortest breakthrough time; thus, M′MOF-**4a** exhibits the highest C_2H_2/C_2H_4 separation capacity. Such different separation capacities are mainly determined by their different porosities and C_2H_2 uptake capacity in which M′MOF-**4a** has the highest, and M′MOF-**7a**, the lowest.

The economics of a PSA unit will be dictated primarily by the amount of C_2H_2 captured during the adsorption cycle, i.e. during the time interval $0-\tau_{break}$. Figure 4d presents plots of the number of millimoles of C_2H_2 captured per liter of adsorbent against the breakthrough time, τ_{break}. It is remarkable to note that per liter of adsorbent material, the number of millimoles of C_2H_2 captured is perfectly linearly related to the dimensionless breakthrough time. This is a rational result. The breakthrough calculations for M′MOFs were performed with the *same volume* of adsorber, containing *identical volumes* of adsorbent materials. Expressed differently, Figure 4d demonstrates that the proper

dx.doi.org/10.1021/ja302380x | J. Am. Chem. Soc. 2012, 134, 8703−8710

metric that determines the separation characteristics of a PSA adsorber is the dimensionless breakthrough time, τ_{break}, which in turn depends on both selectivity and capacity metrics.

CONCLUSION

The metalloligand approach for the construction of porous mixed-metal−organic frameworks (M′MOFs) has been developed to systematically tune the pore spaces by the interplay of both metalloligands and organic linkers in resulting isostructural M′MOFs. Such fine-tuning of the micropores is very challenging, while it is very crucial and important to direct their highly selective recognition and thus separation of both chiral and achiral small molecules. Given the fact that some chiral alcohols are important raw materials for the synthesis of some useful pharmaceutical compounds while both acetylene and ethylene are essential raw chemicals for the production of some fine chemicals and polymers, these new M′MOFs might be implemented in these practical applications. Such feasibility has been further realized by the transient breakthrough simulations in which the purity requirement of 40 ppm in the outlet gas can be readily fulfilled by the fixed bed M′MOF-**4a** adsorber.

ASSOCIATED CONTENT

Supporting Information

Crystalloghaphic data for **M′MOF-4**, **M′MOF-6**, TGA, PXRDs, HPLC plots, structural data of four M′MOFs, isotherm fit parameters, gas sorption isotherms and additional figures. This information is available free of charge via the Internet at http://pubs.acs.org.

AUTHOR INFORMATION

Corresponding Author

r.krishna@uva.nl (R.K.); banglin.chen@utsa.edu (B.C.)

Notes

The authors declare no competing financial interest.

ACKNOWLEDGMENTS

This work was supported by the Award AX-1730 (B.C.) and AX-1593 (J.C.Z.) from the Welch Foundation. A portion of this research was conducted at the Center for Nanophase Materials Sciences, which is sponsored at Oak Ridge National Laboratory by the Office of Basic Energy Sciences, U.S. Department of Energy. We thank Dr. Alakesh Bisai (IISER Bhopal) for helpful discussion regarding chiral separation.

REFERENCES

(1) Long, J. R.; Yaghi, O. M. *Chem. Soc. Rev.* **2009**, *38*, 1213.
(2) Zhou, H.-C.; Long, J. R.; Yaghi, O. M. *Chem. Rev.* **2012**, *112*, 673.
(3) Abrahams, B. F.; Hoskins, B. F.; Michail, D. M.; Robson, R. *Nature* **1994**, *369*, 727.
(4) Gardner, G. B.; Venkataraman, D.; Moore, J. S.; Lee, S. *Nature* **1995**, *374*, 792.
(5) Yaghi, O. M.; Li, G.; Li, H. *Nature* **1995**, *378*, 703.
(6) Subramanian, S.; Zaworotko, M. J. *Angew. Chem., Int. Ed.* **1995**, *34*, 2127.
(7) Kondo, M.; Yoshitomi, T.; Seki, K.; Matsuzaka, H.; Kitagawa, S. *Angew. Chem., Int. Ed.* **1997**, *36*, 1725.
(8) Li, H.; Eddaoudi, M.; O'Keeffe, M.; Yaghi, O. M. *Nature* **1999**, *402*, 276.
(9) Chui, S. S.-Y.; Lo, S. M.-F.; Charmant, J. P. H.; Orpen, A. G.; Williams, I. D. *Science* **1999**, *283*, 1148.
(10) Kitagawa, S.; Kondo, M. *Bull. Chem. Soc. Jpn.* **1998**, *71*, 1739.
(11) Kitagawa, S.; Kitaura, R.; Noro, S.-I. *Angew. Chem., Int. Ed.* **2004**, *43*, 2334.
(12) Eddaoudi, M.; Moler, D. B.; Li, H.; Chen, B.; Reineke, T. M.; O'Keeffe, M.; Yaghi, O. M. *Acc. Chem. Res.* **2001**, *34*, 319.
(13) Ferey, G. *Science* **2001**, *291*, 994.
(14) Seo, J. S.; Whang, D.; Lee, H.; Jun, S. I.; Oh, J.; Jeon, Y. J.; Kim, K. *Nature* **2000**, *404*, 982.
(15) Eddaoudi, M.; Kim, J.; Rosi, N.; Vodak, D.; Wachter, J.; O'Keeffe, M.; Yaghi, O. M. *Science* **2002**, *295*, 469.
(16) Zhao, X.; Xiao, B.; Fletcher, A. J.; Thomas, K. M.; Bradshaw, D.; Rosseinsky, M. J. *Science* **2004**, *306*, 1012.
(17) Ferey, G.; Mellot-Draznieks, C.; Serre, C.; Millange, F.; Dutour, J.; Surble, S.; Margiolaki, I. *Science* **2005**, *309*, 2040.
(18) Furukawa, H.; Ko, N.; Go, Y. B.; Aratani, N.; Choi, S. B.; Choi, E.; Yazaydin, A. O.; Snurr, R. Q.; O'Keeffe, M.; Kim, J.; Yaghi, O. M. *Science* **2010**, *329*, 424.
(19) Farha, O. K.; Yazaydın, A. Ö; Eryazici, I; Malliakas, C. D.; Hauser, B. G.; Kanatzidis, M. G.; Nguyen, S. T.; Snurr, R. Q.; Hupp, J. T. *Nature Chem.* **2010**, *2*, 944.
(20) Ma, S.; Sun, D.; Simmons, J. M.; Collier, C. D.; Yuan, D.; Zhou, H.-C. *J. Am. Chem. Soc.* **2008**, *130*, 1012.
(21) Wu, H.; Zhou, W.; Yildirim, T. *J. Am. Chem. Soc.* **2009**, *131*, 4995.
(22) Guo, Z.; Wu, H.; Srinivas, G.; Zhou, Y.; Xiang, S. C.; Chen, Z.; Yang, Y.; Zhou, W.; O'Keeffe, M.; Chen, B. *Angew. Chem., Int. Ed.* **2011**, *50*, 3178.
(23) Wilmer, C. E.; Leaf, M.; Lee, C. Y.; Farha, O. K.; Hauser, B. G.; Hupp, J. T.; Snurr, R. Q. *Nature Chem.* **2012**, *4*, 83.
(24) Chen, B.; Xiang, S. C.; Qian, G. *Acc. Chem. Res.* **2010**, *43*, 1115.
(25) Chen, B.; Liang, C.; Yang, J.; Contreras, D. S.; Clancy, Y. L.; Lobkovsky, E. B.; Yaghi, O. M.; Dai, S. *Angew. Chem., Int. Ed.* **2006**, *45*, 1390.
(26) Caskey, S. R.; Wong-Foy, A. G.; Matzger, A. J. *J. Am. Chem. Soc.* **2008**, *130*, 10870.
(27) Ma, L.; Falkowski, J. M.; Abney, C.; Lin, W. *Nature Chem.* **2010**, *2*, 838.
(28) Das, M. C.; Bharadwaj, P. K. *J. Am. Chem. Soc.* **2009**, *131*, 10942.
(29) Zhang, Y.-B.; Zhou, H.-L.; Lin, R.-B.; Zhang, C.; Lin, J.-B.; Zhang, J.-P.; Chen, X.-M. *Nat. Commun.* **2012**, *3*, 642.
(30) Vaidhyanathan, R.; Iremonger, S. S.; Shimizu, G. K. H.; Boyd, P. G.; Alavi, S.; Woo, T. K. *Science* **2010**, *330*, 650.
(31) Jeong, N. C.; Samanta, B.; Lee, C. Y.; Farha, O. K.; Hupp, J. T. *J. Am. Chem. Soc.* **2012**, *134*, 51.
(32) Lin, X.; Telepeni, I.; Blake, A. J.; Dailly, A.; Brown, C. M.; Simmons, J. M.; Zoppi, M.; Walker, G. S.; Thomas, K. M.; Mays, T. J.; Hubberstey, P.; Champness, N. R.; Schroder, M. *J. Am. Chem. Soc.* **2009**, *131*, 2159.
(33) Thallapally, P. K.; Tian, J.; Kishan, M. R.; Fernandez, C. A.; Dalgarno, S. J.; McGrail, P. B.; Warren, J. E.; Atwood, J. L. *J. Am. Chem. Soc.* **2008**, *130*, 16842.
(34) Wiers, B. M.; Foo, M.-L.; Balsara, N. P.; Long, J. R. *J. Am. Chem. Soc.* **2011**, *133*, 14522.
(35) An, J.; Farah, O. K.; Hupp, J. T.; Pohl, E.; Yeh, J. I.; Rosi, N. L. *Nat. Commun.* **2012**, *3*, 604.
(36) Pramanik, S.; Zheng, C.; Zhang, X.; Emge, T. J.; Li, J. *J. Am. Chem. Soc.* **2011**, *133*, 4153.
(37) Zheng, B.; Bai, J.; Duan, J.; Wojtas, L.; Zaworotko, M. J. *J. Am. Chem. Soc.* **2011**, *133*, 748.
(38) Lin, Q.; Wu, T.; Zheng, S.-T.; Bu, X.; Feng, P. *J. Am. Chem. Soc.* **2012**, *134*, 784.
(39) Bradshaw, D.; Prior, T. J.; Cussen, E. J.; Claridge, J. B.; Rosseinsky, M. J. *J. Am. Chem. Soc.* **2004**, *126*, 6106.
(40) Vaidhyanathan, R.; Bradshaw, D.; Rebilly, J.-N.; Barrio, J. P.; Gould, J. A.; Berry, N. G.; Rosseinsky, M. J. *Angew. Chem., Int. Ed.* **2006**, *45*, 6495.
(41) Dybtsev, D. N.; Nuzhdin, A. L.; Chun, H.; Bryliakov, K. P.; Talsi, E. P.; Fedin, V. P.; Kim, K. *Angew. Chem., Int. Ed.* **2006**, *45*, 916.
(42) Suh, K.; Yutkin, M. P.; Dybtsev, D. N.; Fedin, V. P.; Kim, K. *Chem. Commun.* **2012**, *48*, 513.
(43) Nuzhdin, A. L.; Dybtsev, D. N.; Bryliakov, K. P.; Talsi, E. P.; Fedin, V. P. *J. Am. Chem. Soc.* **2007**, *129*, 12958.

(44) Yuan, G.; Zhu, C.; Xuan, W.; Cui, Y. *Chem.—Eur. J.* **2009**, *15*, 6428.
(45) Liu, Y.; Xuan, W.; Cui, Y. *Adv. Mater.* **2010**, *22*, 4112.
(46) Li, G.; Yu, W.; Cui, Y. *J. Am. Chem. Soc.* **2008**, *130*, 4582.
(47) Xuan, W.; Zhang, M.; Liu, Y.; Chen, Z.; Cui, Y. *J. Am. Chem. Soc.* **2012**, *134*, 6904.
(48) Xie, X.-M.; Zhang, Z.-J.; Wang, Z.-U.; Yuan, L.-M. *J. Am. Chem. Soc.* **2011**, *133*, 11892.
(49) Liu, B.; Shekhah, O.; Arslan, H. K.; Liu, J.; Wöll, C.; Fischer, R. A. *Angew. Chem., Int. Ed.* **2012**, *51*, 807.
(50) Chen, B.; Eddaoudi, M.; Reineke, T. M.; Kampf, J. W.; O'Keeffe, M.; Yaghi, O. M. *J. Am. Chem. Soc.* **2000**, *122*, 11559.
(51) Chen, B.; Eddaoudi, M.; Hyde, S. T.; O'Keeffe, M.; Yaghi, O. M. *Science* **2001**, *291*, 5506.
(52) Kosal, E.; Chou, J.-H.; Wilson, S. R.; Suslick, K. S. *Nat. Mater.* **2002**, *1*, 118.
(53) Hu, A.; Ngo, H. L.; Lin, W. *Angew. Chem., Int. Ed.* **2003**, *42*, 6000.
(54) Hu, A.; Ngo, H. L.; Lin, W. *J. Am. Chem. Soc.* **2003**, *125*, 11490.
(55) Kitaura, R.; Onoyama, G.; Sakamoto, H.; Matsuda, R.; Noro, S.; Kitagawa, S. *Angew. Chem., Int. Ed.* **2004**, *43*, 2684.
(56) Chen, B.; Fronczek, F. R.; Maverick, A. W. *Inorg. Chem.* **2004**, *43*, 8209.
(57) Cho, S.-H.; Ma, B.; Nguyen, S. T.; Hupp, J. T.; Albrecht-Schmitt, T. E. *Chem. Commun.* **2006**, 2563.
(58) Sakamoto, H.; Matsuda, R.; Bureekaew, S.; Tanaka, D.; Kitagawa, S. *Chem.—Eur. J.* **2009**, *15*, 4985.
(59) Chen, B.; Zhao, X.; Putkham, A.; Hong, K.; Lobkovsky, E. B.; Hurtado, E. J.; Fletcher, A. J.; Thomas, K. M. *J. Am. Chem. Soc.* **2008**, *130*, 6411.
(60) Xiang, S. C.; Zhang, Z.; Zhao, C.-G.; Hong, K.; Zhao, X.; Ding, D.-R.; Xie, M.-H.; Wu, C.-D.; Das, M. C.; Gill, R.; Thomas, K. M.; Chen, B. *Nat. Commun.* **2011**, *2*, 204.
(61) Das, M. C.; Xiang, S. C.; Zhang, Z.; Chen, B. *Angew. Chem., Int. Ed.* **2011**, *50*, 10510.
(62) Shultz, A. M.; Sarjeant, A. A.; Farha, O. K.; Hupp, J. T.; Nguyen, S. T. *J. Am. Chem. Soc.* **2011**, *133*, 13252.
(63) Farha, O. K.; Shultz, A. M.; Sarjeant, A. A.; Nguyen, S. T.; Hupp, J. T. *J. Am. Chem. Soc.* **2011**, *133*, 5652.
(64) Zou, C.; Zhang, Z.; Xu, X.; Gong, Q; Li, J.; Wu, C.-D. *J. Am. Chem. Soc.* **2012**, *134*, 87.
(65) Wang, X.-S.; Meng, L.; Cheng, Q.; Kim, C.; Wojtas, L.; Chrzanowski, M.; Chen, Y.-S.; Zhang, X. P.; Ma, S. *J. Am. Chem. Soc.* **2011**, *133*, 16322.
(66) Xie, Z.; Ma, L.; deKrafft, K. E.; Jin, A.; Lin, W. *J. Am. Chem. Soc.* **2010**, *132*, 922.
(67) Kent, C. A.; Mehl, B. P.; Ma, L.; Papanikolas, J. M.; Meyer, T. J.; Lin, W. *J. Am. Chem. Soc.* **2010**, *132*, 12767.
(68) Song, F.; Wang, C.; Falkowski, J. M.; Ma, L.; Lin, W. *J. Am. Chem. Soc.* **2010**, *132*, 15390.
(69) Liu, D.; Huxford, R. C.; Lin, W. *Angew. Chem., Int. Ed.* **2011**, *50*, 3696.
(70) Bloch, E. D.; Britt, D.; Lee, C.; Doonan, C. J.; Uribe-Romo, F. J.; Furukawa, H.; Long, J. R.; Yaghi, O. M. *J. Am. Chem. Soc.* **2010**, *132*, 14382.
(71) Blake, A. J.; Champness, N. R.; Easun, T. L.; Allan, D. R.; Nowell, H.; George, M. W.; Jia, J.; Sun, X.-Z. *Nature Chem.* **2010**, *2*, 688.
(72) He, H.; Xiang, S.; Chen, B. *J. Am. Chem. Soc.* **2011**, *133*, 14570.
(73) Jiang, H.-L.; Tatsu, Y.; Lu, Z.-H.; Xu, Q. *J. Am. Chem. Soc.* **2010**, *132*, 5586.
(74) Gedrich, K.; Senkovska, I.; Klein, N.; Stoeck, U.; Henschel, A.; Lohe, M. R.; Baburin, I. A.; Mueller, U.; Kaskel, S. *Angew. Chem., Int. Ed.* **2010**, *49*, 8489.
(75) Arya, F.; Bouquant, J.; Chuche, J. *Synthesis* **1983**, *11*, 946.
(76) Yang, Z.-H.; Wang, L-X; Zhou, Z.-H.; Zhou, Q.-L.; Tang, C.-C. *Tetrahedron: Asymmetry* **2001**, *12*, 1579.
(77) Mason, J. A.; Sumida, K.; Herm, Z. R.; Krishna, R.; Long, J. R. *Energy Environ. Sci.* **2011**, *3*, 3030.
(78) Crystal data for M′MOF-**4**: $C_{52}H_{52}Cd_3CuN_6O_{16}$, monoclinic, space group C_2, a = 40.537(3) Å, b = 10.1920(8) Å, c = 18.2312(13) Å, β = 95.188(2)°, V = 7501.5(10) Å^3, Z = 4, D_{calc} = 1.255 g/cm^3, μ = 1.172 mm^{-1}, T = 173(2) K, R1 [$I > 2\sigma(I)$] = 0.0673, wR2 (all data) = 0.1965, S = 1.024; M′MOF-**6**: $C_{71}H_{94}Cd_3CuN_{11}O_{21}$, orthorhombic, space group $P2_12_12_1$, a = 10.3562(3) Å, b = 17.8979(5) Å, c = 44.1383 (14) Å, V = 8181.2(4) Å^3, Z = 4, D_{calc} = 1.493 g/cm^3, μ = 1.100 mm^{-1}, T = 173(2) K, R1 [$I > 2\sigma(I)$] = 0.0457, wR2 (all data) = 0.1234, S = 1.020; unit cell for M′MOF-**5**: Orthorhombic, lattice type P, a = 18.4417(13) Å, b = 40.796(3) Å, c = 9.8609(8) Å, V = 7418.8(10) Å^3; unit cell for M′MOF-**7**: Orthorhombic, lattice type I, a = 9.8491(7) Å, b = 18.5655(15) Å, c = 42.196(3) Å, V = 7715.8(10) Å^3.
(79) Myers, A. L.; Prausnitz, J. M. *AIChEJ* **1965**, *11*, 121.
(80) Krishna, R.; van Baten, J. M. *Chem. Eng. J.* **2007**, *133*, 121 and references therein.
(81) Krishna, R.; Long, J. R. *J. Phys. Chem. C* **2011**, *115*, 12941 and references therein.
(82) Walton, K. S.; LeVan, M. D. *Ind. Eng. Chem. Res.* **2003**, *42*, 6938.
(83) Blatov, V. A.; O'Keeffe, M.; Proserpio, D. M. *CrystEngComm* **2010**, *12*, 44.